Single Molecular Adsorption of Terbium(III) Bis-phthalocyaninato (TbPc2) Governed by Two Surface Reconstructions of Perovskite Type SrVO3 Epitaxial Ultrathin Film

doi: info:doi/10.1246/cl.210270

Advance Publication Cover Page

Chemistry Letters

Single molecular adsorption of terbium(III) bis-phthalocyaninato ($TbPc_2$) governed by two surface reconstructions of perovskite type $SrVO_3$ epitaxial ultrathin film

Hirofumi Oka,* Keiichi Katoh, Yoshinori Okada, Daichi Oka, Taro Hitosugi, Masahiro Yamashita, and Tomoteru Fukumura

Advance Publication on the web May 28, 2021

doi:10.1246/cl.210270

Single molecular adsorption of terbium(III) bis-phthalocyaninato ($TbPc_2$) governed by two surface reconstructions of perovskite type $SrVO_3$ epitaxial ultrathin film

Hirofumi Oka,*[1,2] Keiichi Katoh,[3] Yoshinori Okada,[1,4] Daichi Oka,[5] Taro Hitosugi,[1,6]
Masahiro Yamashita,[1,2,5,7] and Tomoteru Fukumura[1,2,5]

[1]*Advanced Institute for Materials Research, Tohoku University, Sendai 980-8577, Japan*
[2]*Core Research Cluster for Materials Science, Tohoku University, Sendai 980-8577, Japan*
[3] *Department of Chemistry, Graduate School of Science, Josai University, Saitama 350-0295, Japan*
[4] *Okinawa Institute of Science and Technology Graduate University, Okinawa 904-0495, Japan*
[5] *Department of Chemistry, Graduate School of Science, Tohoku University, Sendai 980-8578, Japan*
[6]*Department of Chemical Science and Engineering, School of Materials and Chemical Technology, Tokyo Institute of Technology, Tokyo 152-8550, Japan*
[7]*School of Materials Science and Engineering, Nankai University, Tianjin 300350, China*

E-mail: hirofumi.oka.e3@tohoku.ac.jp

Using low temperature scanning tunneling microscopy (STM), we observed a single molecule magnet, Tb^{3+} double decker molecule $TbPc_2$ (Pc = phthalocyaninato), adsorbed on a perovskite type transition metal oxide $SrVO_3$ ultrathin film. $TbPc_2$ molecules adsorbed intact and flat on two surface reconstructions of $SrVO_3$, ($\sqrt{2}\times\sqrt{2}$)-*R*45° and ($\sqrt{5}\times\sqrt{5}$)-*R*26.6°, with different configurations. High resolution STM images revealed that the adsorption configurations were governed by the adatom structure of each surface reconstruction according to the proposed adsorption configurations.

Keywords: Scanning tunneling microscopy, Single-molecule magnet, Perovskite type transition metal oxide

Single molecule magnets (SMMs) are attractive for the application to molecular spintronics and quantum information processing because of their long magnetization relaxation time and quantum tunneling of magnetization.[1–3] The terbium double-decker molecule ($TbPc_2$: terbium(III) bis-phthalocyaninato neutral complex) has been widely investigated as an SMM, and its deposition onto substrates has been easily performed by the sublimation in vacuum.[4–7] Previously, the electronic coupling between $TbPc_2$ and the substrate was reported to be crucial for the magnetization of $TbPc_2$: almost no remanent magnetization of $TbPc_2$ on conducting Cu(100) substrate due to their strong electronic coupling,[8] while large remanent magnetization with open magnetic hysteresis loop of $TbPc_2$ by inserting an insulating MgO layer between $TbPc_2$ and conducting Ag(100) substrate.[9] Therefore, the choice of substrates is important to tailor the magnetization of SMMs via their electronic coupling. However, the deposition of $TbPc_2$ has been performed mostly onto metal substrates.

Strongly correlated perovskite transition metal oxides (TMOs) show exotic quantum phenomena such as high temperature superconductivity and metal-insulator transition.[10] Such strong electronic correlation could change the electronic coupling between $TbPc_2$ and TMO. In addition, their competing orders at the molecular scale between e.g. superconductivity of TMO and magnetism of $TbPc_2$ could provide rich playgrounds for novel molecular electronics and spintronics. Molecular deposition of $TbPc_2$ on perovskite type TMOs has been performed only for $LaSrMnO_3$ film so far.[11] However, adsorption configuration of $TbPc_2$ was not resolved because of the rough film surface

The adsorption configuration has been theoretically investigated for single-decker Pc molecules on various substrates.[12–17] The attractive force between the molecule and the substrate was mainly van der Waals interaction. In addition, electronic hybridization of the out-of-plane benzene π orbitals with the substrate surface as well as chemical bonding between the Pc's central metal ion and the surface atom contributes to the total attractive force.[16,17] In a previous study, CuPc molecule on $SrTiO_3$ substrate with a ($\sqrt{5}\times\sqrt{5}$)-*R*26.6° surface reconstruction was anchored by the surface reconstruction at room temperature, indicating an important role of the surface reconstruction for the adsorption configuration,[18] although the adsorption configuration of CuPc on $SrTiO_3$ has not been resolved.

Perovskite $SrVO_3$ is an archetypal strongly correlated oxide[19,20] and its epitaxial thin film can be obtained by standard ultrahigh vacuum deposition techniques.[21,22] Recently, we performed *in-situ* observation of $SrVO_3$ ultrathin film by using low temperature scanning tunneling microscope (STM), revealing coexistence of ($\sqrt{5}\times\sqrt{5}$)-*R*26.6° and ($\sqrt{2}\times\sqrt{2}$)-*R*45° reconstructions for ultrathin films thinner than 10 unit cells (UC) (~3.8 nm) and a nanoscale metal-insulator transition in the nanowire.[23,24] In this letter, we report observation of $TbPc_2$ molecules on $SrVO_3$ ultrathin films by using low temperature STM to reveal the adsorption configuration of $TbPc_2$ molecules on $SrVO_3$. $TbPc_2$ molecules adsorbed intact on $SrVO_3$, and their adsorption configuration depended on the two surface reconstructions of $SrVO_3$, suggesting a principal role of the surface reconstruction for adsorption configuration of $TbPc_2$ on $SrVO_3$.

Preparation of $TbPc_2$ was described elesewhere.[4] All reagents for synthesizing $TbPc_2$ were purchased from Wako Pure Chemical Industries, Ltd., TCI, Strem Chemicals, Inc. and Sigma-Aldrich Co. LLC., and used without further purification. $SrVO_3$ (001) ultrathin film was epitaxially grown on Nb (0.05wt%)-doped $SrTiO_3$ (001) single crystal substrate (Shinkosha Co., Ltd.) by using pulsed laser deposition with a base pressure of 5×10^{-10} Torr. A nearly single-phase $Sr_2V_2O_7$ polycrystalline target (Kojundo Chemical Laboratory Co., Ltd.) was ablated by KrF excimer

laser (λ = 248 nm) with a pulse frequency of 2 Hz and a laser fluence of 1 J/cm^2. Prior to growth, the substrate was heated at 500 °C for 2 hours under ultrahigh vacuum (UHV) followed by annealing at 1000 °C for 1 hour under an oxygen partial pressure of 2 × 10^{-7} Torr. The ultrathin film was deposited at 800 °C under UHV with a deposition rate of 0.01 UC per pulse, which was determined by reflection high energy electron diffraction intensity oscillations during film deposition.[25] The film thickness was 6 UC, approximately 2.3 nm. The formation of (√5×√5)-*R*26.6° and (√2×√2)-*R*45° reconstructions on the ultrathin film was confirmed by high-resolution STM measurements.[23] Subsequently, $TbPc_2$ molecules were deposited from a quartz crucible onto the ultrathin film at room temperature at a pressure of < 2 × 10^{-9} Torr. The sample was *in-situ* transferred into a STM head and cooled down to a measurement temperature of 4.8 K.[26,27] All STM images were obtained in constant current mode with electrochemically etched W tips.

Figure 1 shows a schematic structure of a $TbPc_2$ molecule. The $TbPc_2$ has a Tb ion sandwiched between two Pc ligands, which are rotated by 45° with respect to each other. The lateral size and height of the molecule were reported to be ~1.6 nm and ~0.4 nm, respectively, for a single crystal of $TbPc_2$.[4]

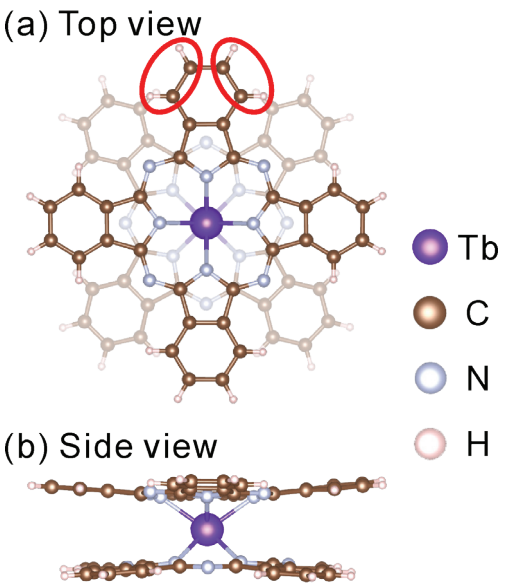

Figure 1. Schematic structure of a terbium double-decker molecule. (a) Top and (b) side views. In the phthalocyanine ligand, its outer edges of benzene ring (red circles) possess high charge distribution.

Figure 2(a) shows a representative STM image of $TbPc_2$ molecules adsorbed on $SrVO_3$ ultrathin film. Two atomically flat terraces of the $SrVO_3$ ultrathin film were observed. High resolution STM images in left and right insets of Figure 2(a) revealed that the lower and upper terraces composed of square lattices with periodicities of 0.55 nm and 0.84 nm corresponds to (√2×√2)-*R*45° and (√5×√5)-*R*26.6° structures, respectively, as was reported previously.[23] $TbPc_2$ molecule was adsorbed separately

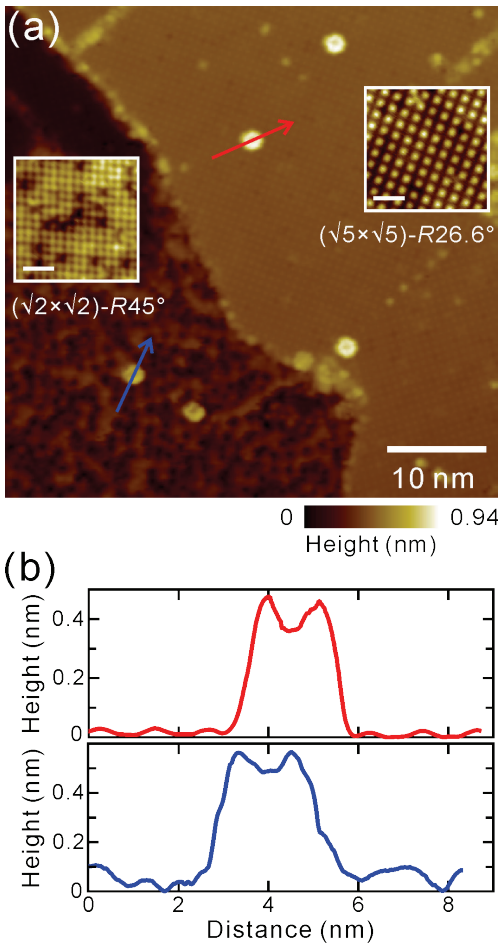

Figure 2. (a) STM image of isolated $TbPc_2$ molecules on $SrVO_3$ ultrathin film. V = 1.5 V, I = 10 pA, and 50×50 nm^2. Left and right insets show high resolution STM images of the lower and upper terraces of the $SrVO_3$ ultrathin film, corresponding to (√2×√2)-*R*45° and (√5×√5)-*R*26.6°structures, respectively. The scale bars = 2 nm. V = 1.5 V, I = 60 pA, and 8×8 nm^2, and V = 0.4 V, I = 20 pA, and 8×8 nm^2 in left and right insets, respectively. (b) Height profiles of the $TbPc_2$ molecules adsorbed on the (√5×√5)-*R*26.6°and the (√2×√2)-*R*45°structures along the red and blue arrows in (a), respectively.

without aggregation both on the (√2×√2)-*R*45° and (√5×√5)-*R*26.6° structures. Figure 2(b) shows height profiles across single $TbPc_2$ molecules on the (√5×√5)-*R*26.6° and (√2×√2)-*R*45° structures. The height of both the $TbPc_2$ molecules was approximately 0.4 nm, which is almost identical with that estimated by X-ray diffraction analysis of $TbPc_2$ single crystal[4] and that of $TbPc_2$ molecule observed by STM.[28,29] Thus, the $TbPc_2$ molecules were adsorbed intact on the $SrVO_3$ ultrathin film, where the Pc ligand planes are parallel to the film surface, similarly to $TbPc_2$ on other substrates.[9,30,31]

To determine adsorption configuration of $TbPc_2$ molecules on $SrVO_3$ ultrathin film, high resolution STM images of $TbPc_2$ were observed. Figure 3(a) shows an STM image of a single $TbPc_2$ molecule on the (√5×√5)-*R*26.6° structure. The molecule was composed of eight lobes with a four-fold symmetry, and the center of the molecule was

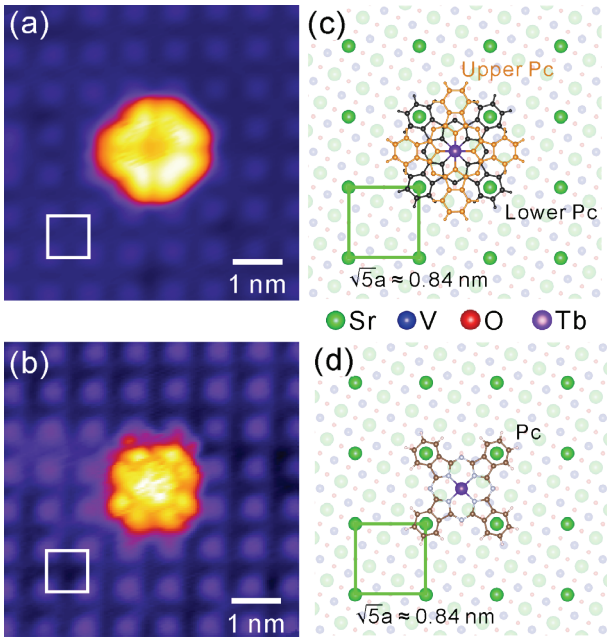

Figure 3. STM images of (a) $TbPc_2$ and (b) single-decker TbPc (or Pc) molecules adsorbed on a (√5×√5)-*R*26.6° structure. V = 1.5 V, I = 10 pA, and 6×6 nm^2. The height of the single-decker molecule was ~0.2 nm, which is a half-height of the $TbPc_2$. The white squares denote the unit cell of the (√5×√5)-*R*26.6° structure of $SrVO_3$. Schematic adsorption configurations of (c) $TbPc_2$ and (d) TbPc molecules on the (√5×√5)-*R*26.6° structure. The upper and lower Pc ligands of $TbPc_2$ are shown in orange and black, respectively. Solid green balls denote Sr adatoms forming the (√5×√5)-*R*26.6° structure on the subsurface atoms in light color. The green square denotes the unit cell of the (√5×√5)-*R*26.6° structure.

located at the hollow site of the (√5×√5)-*R*26.6° square lattice. According to previous density functional theory calculations, the eight lobes structure was attributed to higher charge distribution at two outer edges of each benzene ring in the Pc ligand as indicated by ellipsoids in Figure 1(a).[28,29] The observed $TbPc_2$ molecule predominantly reflected the electronic states of the upper Pc ligand because too far distance between the lower Pc ligand and the STM tip. Therefore, the two diagonally opposite benzene rings of the upper Pc ligand were aligned along the (√5×√5)-*R*26.6° square lattice grid.

This interpretation was supported by STM observation of a single decker molecule adsorbed on a (√5×√5)-*R*26.6° structure of $SrVO_3$ similarly to the lower Pc ligand of $TbPc_2$. Figure 3(b) shows an STM image of the single molecule with a height of ~0.2 nm, which is a half-height of the $TbPc_2$ in Figure 3(a). Since this value was similar to the height reported for single decker Pc molecule,[32–35] the molecule in Figure 3(b) was either TbPc or Pc, which is probably a cracked $TbPc_2$ molecule during the sublimation. The molecule in Figure 3(b) also exhibited eight lobes surrounding the central protrusion at the hollow site of the (√5×√5)-*R*26.6° square lattice. However, the two diagonally opposite benzene rings of the Pc ligand were not parallel to the (√5×√5)-*R*26.6° lattice grid but rotated by 45° with respect to the grid. This result is consistent with the observation of the upper Pc ligand of $TbPc_2$ in Figure 3(a).

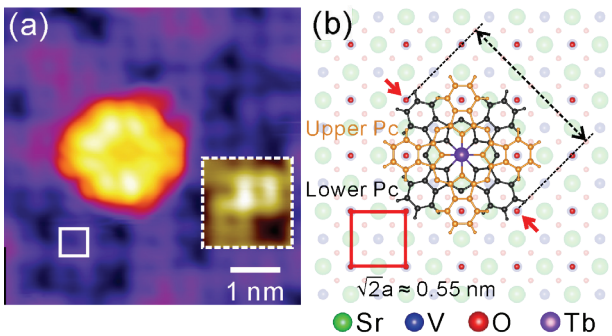

Figure 4. (a) STM image of a single $TbPc_2$ molecule adsorbed on a (√2×√2)-*R*45° structure. V = 1.5 V, I = 50 pA, and 6×6 nm^2. The image contrast is enhanced within the inset using a different color scale for better visibility of the (√2×√2)-*R*45° structure. The white square denotes the unit cell of the (√2×√2)-*R*45° structure of $SrVO_3$. (b) Schematic adsorption configuration of $TbPc_2$ on the (√2×√2)-*R*45° structure. The upper and lower Pc ligands of $TbPc_2$ are shown in orange and black, respectively. Solid red balls denote O adatoms forming the (√2×√2)-*R*45° structure on the subsurface atoms in light color. The red square denotes the unit cell of the (√2×√2)-*R*45° structure. The black dashed arrow corresponds to the lateral size of the lower Pc ligand (~1.6 nm). The distance between two O adatoms along the red arrows is ~1.56 nm.

Figures 3(c) and 3(d) show adsorption configuration models of the $TbPc_2$ and the TbPc molecules on the (√5×√5)-*R*26.6° structure, respectively, based on the above observations. In the (√5×√5)-*R*26.6° lattice, the protrusions observed in Figures 3(a) and 3(b) correspond to Sr adatoms as was reported previously.[23] Therefore, the central Tb ion of the $TbPc_2$ was located at the hollow site of the (√5×√5)-*R*26.6° lattice composed of the Sr adatoms. The benzene ring centers of the lower Pc ligand were located exactly above the Sr adatom sites as shown in Figure 3(c). This adsorption configuration is reasonable since the benzene ring centers have been observed to adsorb atop of the surface atoms, for example, S atoms of MoS_2[36] and Cu atoms of Cu(110).[37,38]

Figure 4(a) shows a high resolution STM image of a single $TbPc_2$ molecule on the (√2×√2)-*R*45° structure. The molecule exhibited eight lobes with a four-fold symmetry, similarly to the one adsorbed on the (√5×√5)-*R*26.6° structure in Figure 3(a). The two diagonally opposite benzene rings of the upper Pc ligand in $TbPc_2$ were aligned parallel to the (√2×√2)-*R*45° square lattice grid, as was observed for the $TbPc_2$ molecule on the (√5×√5)-*R*26.6° structure. Also, the molecule center of $TbPc_2$ was located at a protrusion site of the (√2×√2)-*R*45° lattice, which is composed of O adatoms.[25] From this observation, an adsorption configuration model of the $TbPc_2$ molecule on the (√2×√2)-*R*45° structure are shown in Figure 4(b). In cases of metal phthalocyanines adsorbed on oxides, the central metal ions were often adsorbed atop of surface oxygen atoms to form strong metal-oxygen bonding.[16,39] For $TbPc_2$ in this study, however, the formation of Tb-O bonding was unlikely because the Tb ion was isolated from

the O adatom by the lower Pc ligand of $TbPc_2$ as illustrated in Figure 1(b). Instead, the O adatoms atop of V atoms [Figure 4(b)] might anchor H atoms of the benzene rings in the lower Pc to form V-OH groups, which have been reported to be very stable and easily formed on vanadium oxides surfaces.[40,41] In addition, considering good coincidence between the lateral size of the lower Pc ligand of $TbPc_2$ (~1.6 nm) [a dashed arrow in Figure 4(b)], and the distance between two O adatoms along diagonal direction (~1.56 nm) [red arrows in Figure 4(b)], the adsorption configuration shown in Figure 4(b) would be the most plausible.

In conclusion, we investigated the adsorption configuration of single $TbPc_2$ molecule on $SrVO_3$ ultrathin film at the atomic scale using low temperature STM. $TbPc_2$ molecule was adsorbed on $SrVO_3$ ultrathin film with well-defined adsorption configurations both on the ($\sqrt{5}\times\sqrt{5}$)-*R*26.6° and ($\sqrt{2}\times\sqrt{2}$)-*R*45° structures, suggesting a principal role of the surface reconstruction in the adsorption configuration of $TbPc_2$ on perovskite type TMOs. Since the ($\sqrt{5}\times\sqrt{5}$)-*R*26.6° and ($\sqrt{2}\times\sqrt{2}$)-*R*45° structures exhibited different electronic states,[23] further investigations using scanning tunneling spectroscopy will provide important information to understand electronic coupling between $TbPc_2$ and substrate.[42]

This study was supported by JSPS KAKENHI (Nos. 18H03876, 20H04624, 21H01803, 24750119 and 15K05467) and the WPI-AIMR's fusion research program under World Premier International Research Center Initiative (WPI). M.Y. thanks the support of the 111 project (B18030) from China.

References

1 W. Wernsdorfer, R. Sessoli, *Science* **1999**, *284*, 133.

2 L. Bogani, W. Wernsdorfer, *Nat. Mater.* **2008**, *7*, 179.

3 S. Thiele, F. Balestro, R. Ballou, S. Klyatskaya, M. Ruben, W. Wernsdorfer, *Science* **2014**, *344*, 1135.

4 K. Katoh, Y. Yoshida, M. Yamashita, H. Miyasaka, B. K. Breedlove, T. Kajiwara, S. Takaishi, N. Ishikawa, H. Isshiki, Y. F. Zhang, T. Komeda, M. Yamagishi, J. Takeya, *J. Am. Chem. Soc.* **2009**, *131*, 9967.

5 V. Corradini, A. Candini, D. Klar, R. Biagi, V. De Renzi, A. Lodi Rizzini, N. Cavani, U. del Pennino, S. Klyatskaya, M. Ruben, E. Velez-Fort, K. Kummer, N. B. Brookes, P. Gargiani, H. Wende, M. Affronte, *Nanoscale* **2018**, *10*, 277.

6 S. Müllegger, S. Tebi, A. K. Das, W. Schöfberger, F. Faschinger, R. Koch, *Phys. Rev. Lett.* **2014**, *113*, 133001.

7 A. Lodi Rizzini, C. Krull, T. Balashov, A. Mugarza, C. Nistor, F. Yakhou, V. Sessi, S. Klyatskaya, M. Ruben, S. Stepanow, P. Gambardella, *Nano Lett.* **2012**, *12*, 5703.

8 S. Stepanow, J. Honolka, P. Gambardella, L. Vitali, N. Abdurakhmanova, T.-C. Tseng, S. Rauschenbach, S. L. Tait, V. Sessi, S. Klyatskaya, M. Ruben, K. Kern, *J. Am. Chem. Soc.* **2010**, *132*, 11900.

9 C. Wäckerlin, F. Donati, A. Singha, R. Baltic, S. Rusponi, K. Diller, F. Patthey, M. Pivetta, Y. Lan, S. Klyatskaya, M. Ruben, H. Brune, J. Dreiser, *Adv. Mater.* **2016**, *28*, 5195.

10 Y. Tokura, N. Nagaosa, *Science* **2000**, *288*, 462.

11 L. Malavolti, L. Poggini, L. Margheriti, D. Chiappe, P. Graziosi, B. Cortigiani, V. Lanzilotto, F. B. de Mongeot, P. Ohresser, E. Otero, F. Choueikani, P. Sainctavit, I. Bergenti, V. A. Dediu, M. Mannini, R. Sessoli, *Chem. Commun.* **2013**, *49*, 11506.

12 J. D. Baran, J. A. Larsson, *J. Phys. Chem. C* **2013**, *117*, 23887.

13 M. Endlich, S. Gozdzik, N. Néel, A. L. da Rosa, T. Frauenheim, T. O. Wehling, J. Kröger, *J. Chem. Phys.* **2014**, *141*, 184308.

14 P. Castro-Latorre, S. Miranda-Rojas, F. Mendizabal, *RSC Adv.* **2020**, *10*, 3895.

15 L. Buimaga-Iarinca, C. Morari, *Sci. Rep.* **2018**, *8*, 12728.

16 T. Schmitt, P. Ferstl, L. Hammer, M. A. Schneider, J. Redinger, *J. Phys. Chem. C* **2017**, *121*, 2889.

17 G. Mattioli, F. Filippone, P. Alippi, P. Giannozzi, A. A. Bonapasta, *J. Mater. Chem.* **2012**, *22*, 440.

18 H. Tanaka, T. Kawai, *Jpn. J. Appl. Phys.* **1996**, *35*, 3759.

19 T. Yoshida, M. Kobayashi, K. Yoshimatsu, H. Kumigashira, A. Fujimori, *J. Electron Spectros. Relat. Phenomena* **2016**, *208*, 11.

20 M. Brahlek, L. Zhang, J. Lapano, H.-T. Zhang, R. Engel-Herbert, N. Shukla, S. Datta, H. Paik, D. G. Schlom, *MRS Commun.* **2017**, *7*, 27.

21 M. Takizawa, M. Minohara, H. Kumigashira, D. Toyota, M. Oshima, H. Wadati, T. Yoshida, A. Fujimori, M. Lippmaa, M. Kawasaki, H. Koinuma, G. Sordi, M. Rozenberg, *Phys. Rev. B* **2009**, *80*, 235104.

22 K. Yoshimatsu, T. Okabe, H. Kumigashira, S. Okamoto, S. Aizaki, A. Fujimori, M. Oshima, *Phys. Rev. Lett.* **2010**, *104*, 147601.

23 H. Oka, Y. Okada, T. Hitosugi, T. Fukumura, *Appl. Phys. Lett.* **2018**, *113*, 171601.

24 H. Oka, Y. Okada, K. Kaminaga, D. Oka, T. Hitosugi, T. Fukumura, *Appl. Phys. Lett.* **2020**, *117*, 051603.

25 Y. Okada, S.-Y. Shiau, T.-R. Chang, G. Chang, M. Kobayashi, R. Shimizu, H.-T. Jeng, S. Shiraki, H. Kumigashira, A. Bansil, H. Lin, T. Hitosugi, *Phys. Rev. Lett.* **2017**, *119*, 86801.

26 K. Iwaya, R. Shimizu, T. Hashizume, T. Hitosugi, *Rev. Sci. Instrum.* **2011**, *82*, 083702.

27 K. Iwaya, T. Ohsawa, R. Shimizu, Y. Okada, T. Hitosugi, *Sci. Technol. Adv. Mater.* **2018**, *19*, 282.

28 L. Vitali, S. Fabris, A. M. Conte, S. Brink, M. Ruben, S. Baroni, K. Kern, *Nano Lett.* **2008**, *8*, 3364.

29 T. Komeda, H. Isshiki, J. Liu, Y.-F. Zhang, N. Lorente, K. Katoh, B. K. Breedlove, M. Yamashita, *Nat. Commun.* **2011**, *2*, 217.

30 A. Lodi Rizzini, C. Krull, A. Mugarza, T. Balashov, C. Nistor, R. Piquerel, S. Klyatskaya, M. Ruben, P. M. Sheverdyaeva, P. Moras, C. Carbone, C. Stamm, P. S. Miedema, P. K. Thakur, V. Sessi, M. Soares, F. Yakhou-Harris, J. C. Cezar, S. Stepanow, P. Gambardella, *Surf. Sci.* **2014**, *630*, 361.

31 F. Ara, H. Oka, Y. Sainoo, K. Katoh, M. Yamashita, T. Komeda, *J. Appl. Phys.* **2019**, *125*, 183901.

32 X. Lu, K. W. Hipps, X. D. Wang, U. Mazur, *J. Am. Chem. Soc.* **1996**, *118*, 7197.

33 X. Lu, K. W. Hipps, *J. Phys. Chem. B* **1997**, *101*, 5391.

34 C. Iacovita, M. V. Rastei, B. W. Heinrich, T. Brumme, J. Kortus, L. Limot, J. P. Bucher, *Phys. Rev. Lett.* **2008**, *101*, 116602.

35 N. Tsukahara, K. Noto, M. Ohara, S. Shiraki, N. Takagi, Y. Takata, J. Miyawaki, M. Taguchi, A. Chainani, S. Shin, M. Kawai, *Phys. Rev. Lett.* **2009**, *102*, 167203.

36 A. J. Fisher, P. E. Blöchl, *Phys. Rev. Lett.* **1993**, *70*, 3263.

37 A. Garlant, B. Maughan, P. Zahl, O. L. A. Monti, *Surf. Sci.* **2020**, *696*, 121590.

38 Q. Chen, A. J. McDowall, N. V. Richardson, *Langmuir* **2003**, *19*, 10164.

39 J. Guo, X. Yan, Q. Liu, Q. Li, X. Xu, L. Kang, Z. Cao, G. Chai, J. Chen, Y. Wang, J. Yao, *Nano Energy* **2018**, *46*, 347.

40 B. Tepper, B. Richter, A.-C. Dupuis, H. Kuhlenbeck, C. Hucho, P. Schilbe, M. A. bin Yarmo, H.-J. Freund, *Surf. Sci.* **2002**, *496*, 64.

41 N. Nilius, V. Simic-Milosevic, *J. Phys. Chem. C* **2008**, *112*, 10027.

42 M. Yamashita, *Bull. Chem. Soc. Jpn.* **2021**, *94*, 209.